

STUDY OF A HYDROFLUIDIZATION SYSTEM USING COMPUTATIONAL FLUID DYNAMICS AND A DISCRETE ELEMENT METHOD II: HEAT TRANSFER AND TURBULENCE INTENSITY

J. D. ORONÁ, S. E. ZORRILLA and J. M. PERALTA

Instituto de Desarrollo Tecnológico para la Industria Química (INTEC). Universidad Nacional del Litoral – CONICET. Güemes 3450, S3000GLN. Santa Fe. Argentina.
E-mail: jmperalta@intec.unl.edu.ar

ABSTRACT. Hydrofluidization (HF) is a method of chilling and freezing of foods that pumps a refrigerating liquid upwards through orifices into a vessel creating submerged jets and thus results in extremely high surface transfer phenomena. The objective was to model the heat transfer and turbulence intensity in a HF system with spheres through computational fluid dynamics and a discrete element method. The HF system and the operative variables were those used in a companion paper presented as Part I. The independence of the mesh was checked. The heat transfer model was validated using data from a previous study with static spheres. The results were in the range of experimental data obtained in similar conditions. The model proposed provides useful information about the relationship between the operative variables and the heat transfer and turbulence levels in a HF system.

1. INTRODUCTION

Hydrofluidization (HF) is a method of chilling and freezing of foods that pumps a refrigerating liquid upwards through orifices into a vessel creating submerged jets and thus results in extremely high surface transfer phenomena (Fikiin, 1992; Peralta *et al.*, 2012). Under controlled conditions, it represents an attractive industrial method with advantages related to the small equipment used and the improvement of the freezing of individual pieces of food, besides the advantages related to the immersion chilling and freezing process (ICF).

As stated in the companion Part I (Oroná *et al.*, 2014), several experimental and theoretical studies on HF were conducted using different operative and geometric variables configuration. Although these studies showed the effect of the main variables on momentum, heat and mass transfers, most of them used simple configuration and limited descriptions were carried out. Thus, studies with several food samples are necessary.

A method for modeling moving objects in fluid systems is to combine computational fluid dynamics (CFD) with a discrete phase (DPM) (Fluent, 2011) and element (DEM) (Cundall and Strack, 1979) methods. A DEM consists in performing momentum balances for each particle to estimate the velocity and position within a domain. These balances take into account different interaction forces such as fluid–particle drag, particle–particle collisions, particle–wall collisions, etc. Some of these forces are also balanced with the fluid movement

solved through Navier–Stokes and continuity balances (Fluent, 2011). The main advantages of this technique is that relatively good predictions can be made using low computational efforts compared to systems were fluid to particle interactions (SFI) with moving meshes are used (Fluent, 2011). However, it is important to mention that the volume fraction of the solids must be lower than 12% and heat transfer due to particle–particle collisions are not estimated (Fluent, 2011).

The objective of this work was to model the heat transfer and the turbulence intensity using spheres in a HF system through computational fluid dynamics and a discrete element method. The flow fields and the sphere velocities are studied in a companion paper (Part I) (Oroná *et al.*, 2014).

2. MATERIALS AND METHODS

2.1. Studied System and Conditions

The hydrofluidization (HF) system and the studied conditions were those used in Part I (Oroná *et al.*, 2014). Briefly, the HF system consisted in a cylindrical vessel containing a square arrangement of 13 potato (*Solanum tuberosum* L.) spheres (food product) of 10-mm diameter placed initially at 3-cm height (Figure 1a). The operative variables used were: the refrigerant temperature ($T = -5^{\circ}\text{C}$ and $T = -10^{\circ}\text{C}$), the average fluid velocity at the orifices ($V = 0.59 \text{ m s}^{-1}$ and $V = 1.18 \text{ m s}^{-1}$) and the distance between the geometrical center of the spheres ($S = 1 \text{ cm}$ and $S = 2 \text{ cm}$) (Figure 1b,c). The liquid refrigerant was considered as an aqueous solution of NaCl 0.231 kg kg^{-1} (w/w) (Peralta *et al.*, 2012). A total of 8 conditions were used. These conditions were codified for example: the code T10V059S2 means $T = -10^{\circ}\text{C}$, $V = 0.59 \text{ m s}^{-1}$ and $S = 2 \text{ cm}$.

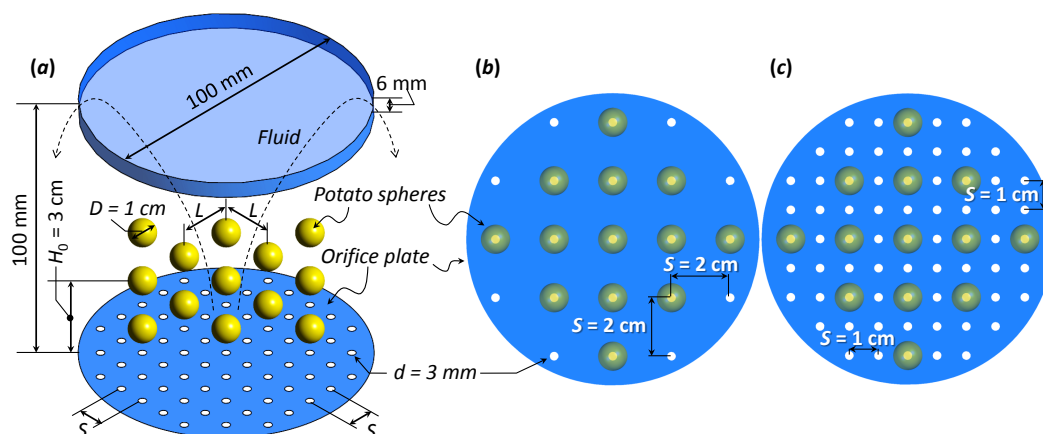


Figure 1 – (a) Scheme of the studied HF system (physical domain) and arrangements (top view) used for the orifices and the spheres (initial). (b) $S = 2 \text{ cm}$ (21 orifices) and (c) $S = 1 \text{ cm}$ (69 orifices). $L = 2 \text{ cm}$.

2.2. Mathematical Modeling

The flow field and the absolute and relative velocities of the spheres were modeled, in Part I (Oroná *et al.*, 2014), by solving mass (continuity) and momentum (Navier-Stokes)

balances for the refrigerant liquid and momentum balances using discrete phase method (DPM) and discrete element method (DEM) for the spheres. The turbulence effect was estimated by the two parameter κ - ω Shear Stress Transport (SST) model (Fluent, 2011).

The heat transfer between the refrigerant liquid and the spheres was estimated by Equation (1) which is an empirical correlation of average Nusselt, Reynolds and Prandtl numbers (Green and Perry, 2008; Fluent, 2011).

$$Nu_D = 2 + \left(0.4 Re_D^{1/2} + 0.06 Re_D^{2/3}\right) Pr^{0.4} (\mu/\mu_s)^{1/4} \quad (1)$$

where Nu_D is the average Nusselt number based on the sphere diameter ($h_c D/k$) [-], Re_D is the Reynolds number based on the sphere diameter ($\rho D v_{slip}/\mu$) [-], Pr is the Prandtl number ($C_p \mu/k$) [-], μ is the refrigerant viscosity [Pa s], μ_s is the refrigerant viscosity at the sphere surface [Pa s], h_c is the surface heat transfer coefficient [$W m^{-2} K^{-1}$], D is the sphere diameter [m], k is the refrigerant thermal conductivity [$W m^{-2} K^{-1}$], ρ is the refrigerant density [$kg m^{-3}$], v_{slip} is the slip velocity of the spheres [$m s^{-1}$] calculated in Part I (Oroná *et al.*, 2014) and C_p is the refrigerant heat capacity [$J kg^{-1} K^{-1}$]. Equation (1) is valid for $0.7 < Pr < 380$, $3.5 < Re < 8 \times 10^4$ and $1 < \mu/\mu_s < 3.2$ (Green and Perry, 2008). It is important to mention that the sphere temperature used in the calculation of μ_s was estimated as the average of the initial temperature of the sphere and the refrigerant temperature.

2.3. Computational Domain and Analyzed Variables

The computational domain was presented in Part I (Oroná *et al.*, 2014). Briefly, a 6-mm slit at the top of the cylindrical wall was used as a fluid exit (Figure 1). Solid walls were assumed to be adiabatic and the system pressure was 0.1 MPa. A 1/7th power velocity profile was used in the round orifice because a fully turbulent liquid-jet with a turbulence intensity of 5% was assumed. The domain was discretized by a mesh composed by tetrahedral elements, which was denser near the orifices.

Each condition (Table 1) was simulated up to 8 s. In the first 3 s, only the momentum and mass balances in the fluid were simulated to reach steady state conditions in the flow field. After $t = 3$ s, the spheres were injected and the following 5 s were used to simulate their movements and interactions inside the domain.

The momentum and mass balances for the fluid and the spheres (Navier–Stokes, continuity, DPM and DEM) were solved using the commercial CFD software ANSYS–ICEM–CFD 14.1 and ANSYS–FLUENT 14.1 (ANSYS Inc., Canonsburg, USA). The simulations were carried out using a PC with an Intel core i7 3930 processor of 3.2 GHz with 16 GB of RAM (DDR3 1600 MHz). Each simulation took approximately 90 h to converge.

Representative variables were used to study the heat transfer and turbulence intensities. These variables were the volume-averaged turbulence intensity $\langle Tu \rangle$ (Equation (2)), the volume-averaged surface heat transfer coefficient $\langle h_c \rangle$ (Equation (3)) and the time-averaged of Equation (3) $\langle \langle h_c \rangle \rangle$ (Equation (4)).

$$\langle Tu \rangle = V_T^{-1} \int_{V_T} Tu \, dV \quad (2)$$

$$\langle h_c \rangle = V_T^{-1} \int_{V_T} h_c dV \quad (3)$$

$$\langle \langle h_c \rangle \rangle = t_{Res}^{-1} \int_{t_{Res}} \langle h_c \rangle dt \quad (4)$$

where Tu is the local turbulence intensity [-], h_c is the local surface heat transfer coefficient [$\text{W m}^{-2} \text{K}^{-1}$], V_T is the domain volume [m^3] (including liquid and spheres) and t_{Res} is the total residence time of the spheres in the domain [s].

2.4. Model Validation

As stated in Part I (Oroná *et al.*, 2014), the mathematical model was partially validated using heat transfer data from Belis *et al.* (2012) for a similar HF configuration but using static spheres (considered as a reference case because h_c was obtained from boundary layer data).

3. RESULTS AND DISCUSSION

3.1. Independence Test and Model Validation

A mesh independence test was carried out testing 6 different mesh compositions (from 86296 to 170770 tetrahedra) using profiles of $\langle Tu \rangle$ and $\langle h_c \rangle$ at $t = 3$ s for the condition T5V118S1. Based on this procedure and taking into account the velocity profiles checked in Part I (Oroná *et al.*, 2014), a mesh composed by 170770 tetrahedra was used for the simulations. It is important to mention that in order to minimize convergence problems, a mesh with elements of the same or greater size than the spheres were considered in the selection procedure (Fluent, 2011). Figure 2 shows the velocity profiles for the meshes checked.

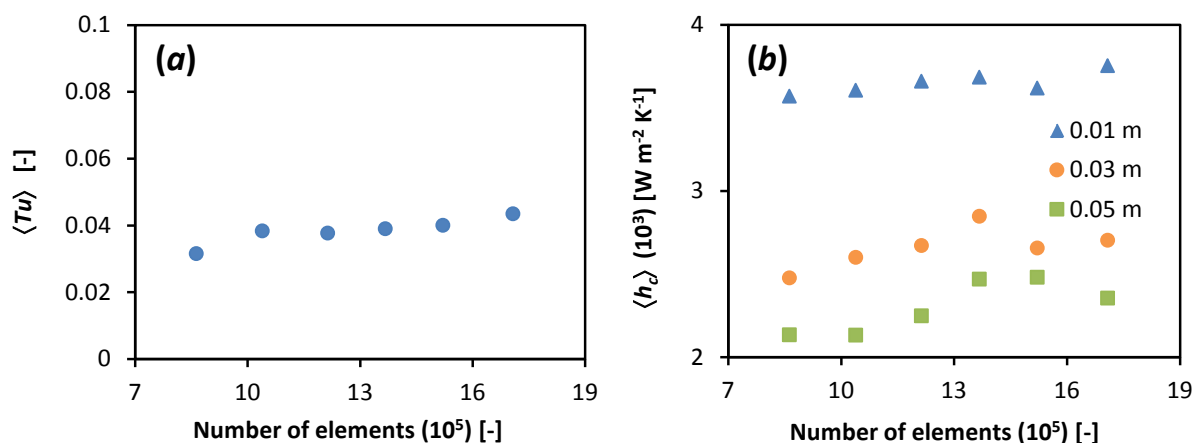


Figure 2 – Mesh independence test using values of (a) $\langle Tu \rangle$ and (b) $\langle h_c \rangle$ as a function of the number of elements. The condition used was T5V118S1.

The validation step was carried out by comparing the values of area-averaged surface heat transfer coefficient (h_c) calculated at $t = 3$ s using Equation (1) with those obtained by Belis *et al.* (2012) using a square arrangement of 13 static spheres of 2-cm diameter, separated by 2 cm and placed at 1 and 5 cm away from the orifice plate. In total, 8 conditions

were used in a range of $1000 \text{ W m}^{-2} \text{ K}^{-1} < h_c < 5000 \text{ W m}^{-2} \text{ K}^{-1}$. Figure 3 shows the compared values of h_c . A mean percent error of 13% was obtained which was considered as very good.

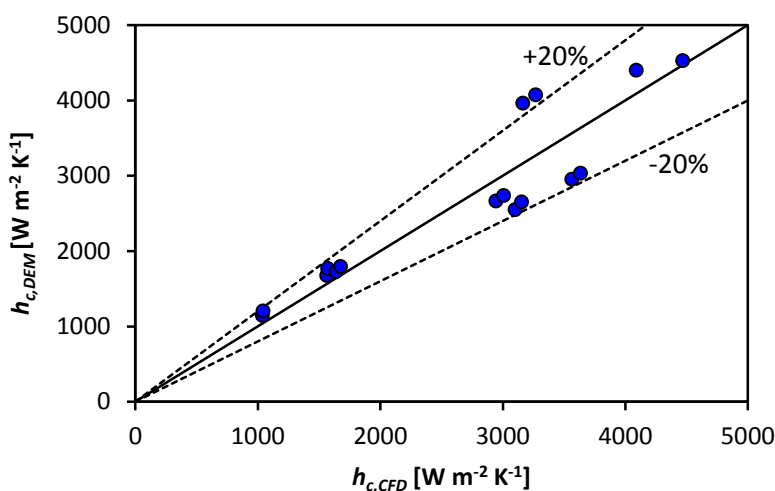


Figure 3 – Comparison between values of h_c calculated using Equation (1) ($h_{c,DEM}$) and that reported by [Belis et al. \(2012\)](#) ($h_{c,CFD}$). Dashed lines represent a mean percent error of $\pm 20\%$.

3.2. Turbulence Intensity

The effect of the operative variables on the turbulence intensity was studied using a relative turbulence intensity parameter ($\langle Tu \rangle_{rel}$) evaluated at $t = 4 \text{ s}$ (*i.e.* 1 s after the injection of the spheres). This parameter was calculated as $\langle Tu \rangle_{rel} / \langle Tu \rangle_{ref}$, where $\langle Tu \rangle_{ref}$ is the reference turbulence intensity calculated for the condition with the smaller value of $\langle Tu \rangle$ at $t = 4 \text{ s}$ (*i.e.* T5V059S2). Figure 4 shows the values of $\langle Tu \rangle_{rel}$ for the studied conditions.

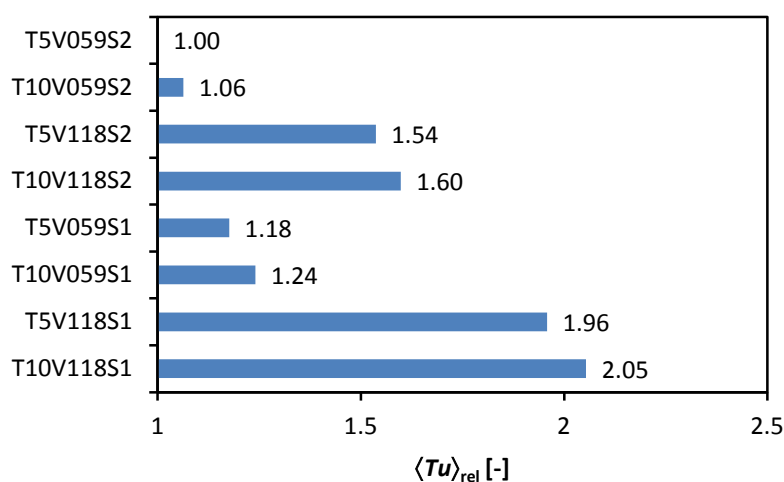


Figure 4 – Values of $\langle Tu \rangle_{rel}$ for the studied conditions.

In general, the variable that most affected $\langle Tu \rangle_{rel}$ was V , followed by S and T . An increase in V and a decrease in S and T lead to an increase in $\langle Tu \rangle_{rel}$. An increment of 0.59 m

s^{-1} in V produced an increment of 60% in $\langle Tu \rangle_{rel}$, while, a decrease of 1 cm in S produced an increase of 20% in $\langle Tu \rangle_{rel}$. Finally, an increase of $\langle Tu \rangle_{rel}$ of 5% was observed for a decrease of $5^\circ C$ in T .

3.3. Surface Heat Transfer Coefficient

Figure 5 shows the $\langle h_c \rangle$ profiles as a function of time for the studied conditions and a range of $3\text{ s} < t < 4\text{ s}$. In general, those profiles presented a similar shape to the $\langle v_{slip} \rangle$ profiles of Part I (Oroná *et al.*, 2014). In addition, the operative variables affected $\langle h_c \rangle$ in a similar way to that observed for $\langle v_{slip} \rangle$. Equation (1) clearly shows direct effect of $\langle v_{slip} \rangle$ on $\langle h_c \rangle$. A range of $800\text{ W m}^{-2}\text{ K}^{-1} < \langle h_c \rangle < 4000\text{ W m}^{-2}\text{ K}^{-1}$ was observed. This result shows the large variability of $\langle h_c \rangle$ on the surface of the spheres moving through the domain.

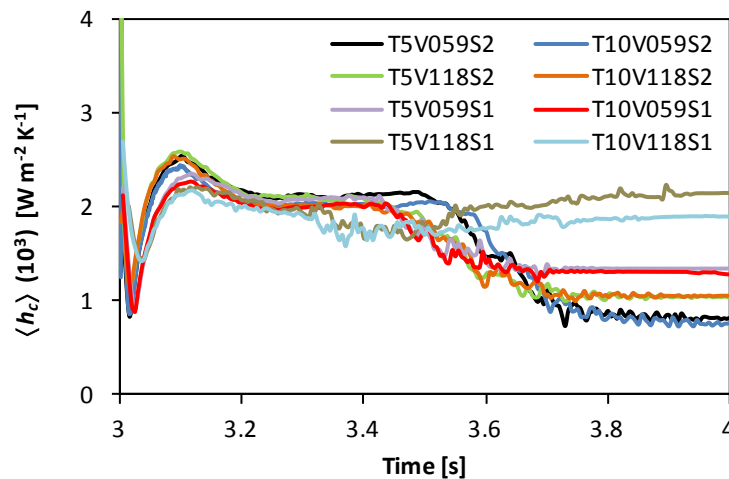


Figure 5 – Profiles of $\langle h_c \rangle$ as a function of time for the studied conditions.

The stochastic movement of the spheres induced by the fluid flow and the buoyancy requires the use time-independent parameters to represent each condition. In this case, the time-volume-averaged surface heat transfer coefficient $\langle\langle h_c \rangle\rangle$ (Equation (4)) was used, where $t_{Res} = t_{final} - t_{injection} = 5\text{ s}$. Table 1 shows the values of $\langle\langle h_c \rangle\rangle$ for the studied conditions. In general, an increase in V (*i.e.* mass flow rate) and a decrease in S and T produced a decrease in $\langle\langle h_c \rangle\rangle$. This behavior is similar to that observed for $\langle h_c \rangle$. Approximately, the changes in the operative variables produced variations on $\langle\langle h_c \rangle\rangle$ of 60% for V , 35% for S and 5% for T .

Table 1 – Values of $\langle\langle h_c \rangle\rangle$ for the studied conditions.

| Condition | $\langle\langle h_c \rangle\rangle [\text{W m}^{-2}\text{ K}^{-1}]$ | Condition | $\langle\langle h_c \rangle\rangle [\text{W m}^{-2}\text{ K}^{-1}]$ |
|-----------|---|-----------|---|
| T5V059S2 | 981 | T5V059S1 | 1414 |
| T10V059S2 | 910 | T10V059S1 | 1349 |
| T5V118S2 | 1171 | T5V118S1 | 2104 |
| T10V118S2 | 1165 | T10V118S1 | 1908 |

4. CONCLUSIONS

A study of the effect of operational variables (flow rate and temperature) and the number of orifices, on the heat transfer and turbulence intensity that occurs between moving spheres and the refrigerant in a HF system was performed. This was carried out using a mathematical model that solved Navier–Stokes and continuity with CFD and the mobility of spheres using discrete phase (DPM) and discrete element methods (DEM). Representative variables such as velocity contours and streamlines for the fluid and absolute and relative velocity profiles for the spheres were used to study the transfers. In general, S was the most significant parameter followed by V . The refrigerant temperature had a marginal effect on the studied transfers.

This study, along with Part I, shows that the combination of CFD with DPM and DEM can be a powerful tool to simulate and study real HF systems with a minimum computational requirement compared to other approaches such as solid-fluid interaction studies.

5. REFERENCES

- BELIS, E. E.; ZORRILLA, S. E.; PERALTA, J. M. Fenómenos de transporte en un sistema de hidrofluidización afectado por el número de orificios y las variables operativas. In: IV Congreso Internacional de Ciencia y Tecnología de los Alimentos (CICYTAC 2012), Nov. 14–16, Córdoba, Argentina, 2012.
- CUNDALL, P. A.; STRACK, D. L. A discrete numerical model for granular assemblies. *Géotechnique*, v. 29, p. 47–65, 1979.
- FIKIIN, A. G. New method and fluidized water system for intensive chilling and freezing of fish. *Food Control*, v. 3, p. 153–160. 1992.
- FLUENT. *Theory guide. ANSYS-FLUENT 14.1*. Canonsburg: ANSYS Inc., 2011.
- GREEN, D.; PERRY, R. *Perry's chemical engineers' handbook*. Eighth edition. New York: McGraw-Hill, 2008.
- ORONÁ, J. D.; ZORRILLA, S. E.; PERALTA, J. M. Study of a hydrofluidization system using computational fluid dynamics and a discrete element method I: flow field and velocity profiles. In: XX Congresso Brasileiro de Engenharia Química (COBEQ), Oct. 19–22, Florianópolis, Brazil, 2014.
- PERALTA, J. M.; RUBIOLO, A. C.; ZORRILLA, S. E. Mathematical modeling of the heat and mass transfer in a stationary potato sphere impinged by a single round liquid jet in a hydrofluidization system. *J. Food Eng.*, v. 109, p. 501–512, 2012.

Acknowledgments

This research was supported partially by Universidad Nacional del Litoral (Santa Fe, Argentina), Consejo Nacional de Investigaciones Científicas y Técnicas (CONICET), and Agencia Nacional de Promoción Científica y Tecnológica (ANPCyT).